

# *Investigation of Kinetic and Dosimetric Features of Citric Acid Using ESR Spectroscopy*

**H. Tuner**

**Applied Magnetic Resonance**

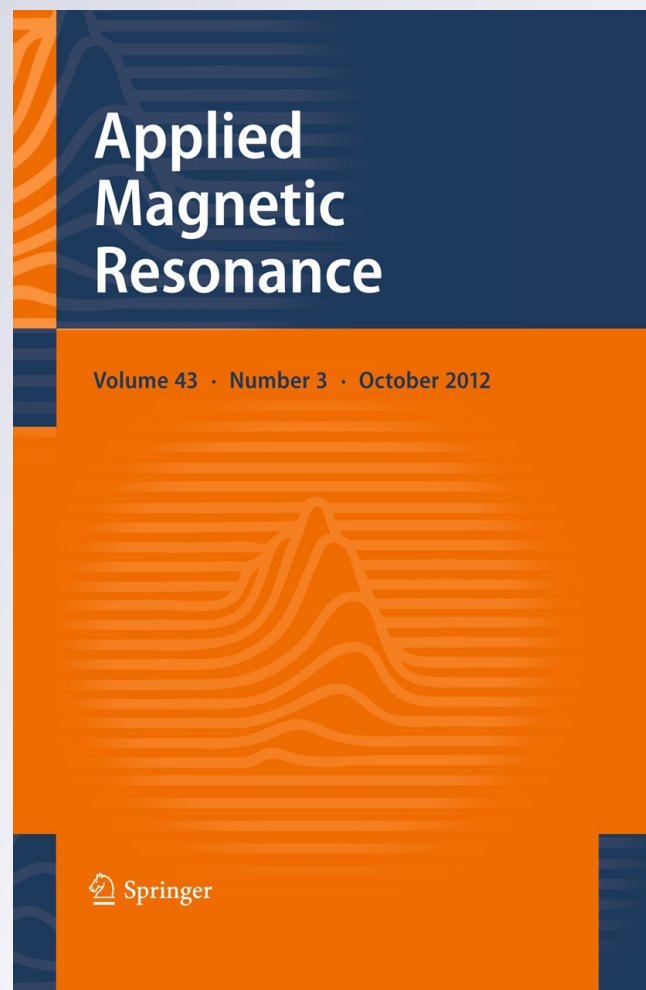
ISSN 0937-9347

Volume 43

Number 3

Appl Magn Reson (2012) 43:363-376

DOI 10.1007/s00723-012-0361-6



**Your article is protected by copyright and all rights are held exclusively by Springer-Verlag. This e-offprint is for personal use only and shall not be self-archived in electronic repositories. If you wish to self-archive your work, please use the accepted author's version for posting to your own website or your institution's repository. You may further deposit the accepted author's version on a funder's repository at a funder's request, provided it is not made publicly available until 12 months after publication.**

# Investigation of Kinetic and Dosimetric Features of Citric Acid Using ESR Spectroscopy

H. Tuner

Received: 20 December 2011 / Revised: 20 March 2012 / Published online: 3 June 2012  
© Springer-Verlag 2012

**Abstract** In the present work, dosimetric potential and temperature-dependent behaviors of the radicals produced upon  $\gamma$ -irradiation of anhydrous and monohydrate citric acid were explored through a detail electron spin resonance (ESR) study. While unirradiated samples presented no ESR signal, irradiated samples were observed to exhibit an ESR spectrum consisting of many intense and weak resonance lines spread over a magnetic field range about 13 mT and centered at  $g = 2.0032$ . Although, the radicals produced upon  $\gamma$ -irradiation have the same structures, the ESR spectra of both compounds of citric acid were observed to be different. An evaluation technique based on the variations of the characteristic resonance lines and the spectrum area was adopted to assign the radical species responsible for the observed experimental ESR spectrum and to determine their kinetic and dosimetric features.

## 1 Introduction

Citric acid (CA) or chemically 2-hydroxy-1,2,3-propanetricarboxylic acid, is a weak organic acid. It is commonly used as a food additive; to make foods tart, to adjust the acidity, to generate carbon dioxide gas, and as an antioxidant to prevent the oils from becoming rancid [1–6]. CA is also used in industry such as plasticizers in plastics industry, detergents, metal cleaning, textile printing and dyeing, and photography [7–12]. CA crystallize into two different forms; the anhydrous CA is monoclinic with a space group of  $P2_{1/a}$  and the monohydrate CA is orthorhombic with a space group of  $P2_12_12_1$ , and both the compounds have four molecules in the unit cell [13–15].

---

H. Tuner (✉)  
Department of Physics, Faculty of Science,  
Balikesir University, Cagis, 10145 Balikesir, Turkey  
e-mail: htuner@balikesir.edu.tr

ESR spectroscopic features of the radicals that produced in X-irradiated CA single crystals at 4.2 and 300 K, and UV-irradiated aqueous solutions of CA and sodium salts of CA at room temperature (RT) were reported previously [16, 17]. Finch et al. [16] performed their investigation on the partially deuterated CA single crystals to identify the H atoms that contribute to the observed hyperfine couplings. They reported that the main radicals observed after irradiation at 4.2 K are radical I and II. The radical I was proposed to be the oxidation species produced by decarboxylation of the central carboxyl group with hyperfine coupling to the four inequivalent  $\beta$ -protons [16]. The same radical was proposed by Zeldes and Livingston [17] to be produced in UV-irradiated aqueous solutions of CA. The other radical (denoted as radical II), that proposed to be produced at 4.2 K by Finch et al., is the anion radical with the unpaired electron that located on one of the end carboxyl groups. However, radical II decays when crystal CA is heated to 300 K and another radical, denoted as radical III, is formed [16]. The radical I and III have been shown by Finch et al. [16] to be the predominant species responsible for the observed RT ESR spectra of partially deuterated CA single crystals. The radical III, which is formed by loss of one of the methylene hydrogen, shows large hyperfine splitting due to an  $\alpha$ -proton and other three protons causing a splitting of less than the observed linewidth of 0.6 mT [16]. The same radical is proposed to be produced in aqueous solutions of CA, but Zeldes and Livingston [17] denoted it as radical II. Another radical of unknown structure and much weaker concentration than I and III, has also been proposed to exist in X-irradiated crystal CA after heating to 300 K [16]. Furthermore, Zeldes and Livingston [17] proposed another radical, which is formed by loss of one of the carboxyl groups was also produced after UV irradiation CA aqueous solutions. The radical notation of Finch et al. was accepted in the present work. Namely, in the present study the radicals I and III which proposed by Finch et al. [16], and the radical that have the same structure as the radical proposed by Zeldes and Livingston [17] were supposed to be formed upon  $\gamma$  irradiation both CA compounds.

While, radiosensitivity and kinetic features of sodium salt of CA were studied in detail in the literature [18], in our knowledge no attempt has been made to determine the kinetic features of the produced radicals, radiosensitivity and possible dosimetric potential of CA. The aim of the present work is to investigate the kinetic features of the radicals produced in  $\gamma$ -irradiated anhydrous and monohydrate CA, and to explore the radiosensitivity and possible dosimetric potential of these compounds through a detail ESR study carried out at different temperatures.

## 2 Materials and Methods

White polycrystalline, anhydrous and monohydrate CA samples were supplied from Vankim Chemistry (Istanbul) and stored at RT (290 K) in a well-closed container. No further purification was performed. All irradiations were performed at RT using a  $^{60}\text{Co}$ - $\gamma$  source supplying a dose rate of 1.6 kGy/h. The dose rate at the sample site was measured by a Fricke dosimeter. Samples irradiated in the dose range of 0.5–20 kGy were employed to construct the dose–response curves. The RT and high

temperature stability and kinetic features of the radiation-induced radicals were investigated using the samples irradiated to a dose of 10 kGy. Annealing studies were performed in the range of 370–410 K and 310–330 K for anhydrous and monohydrate CA, respectively. Samples heated up to predetermined temperatures were kept at these temperatures for predetermined times, and the spectra were recorded at a regular time intervals.

ESR measurements were carried out on samples in standard ESR quartz tubes of 4 mm inner diameter using a Bruker EMX-131 X-band ESR spectrometer operating at  $\sim 9.8$  GHz and equipped with high sensitive cylindrical cavity. The  $g$  value was measured using 2,2-diphenyl-1-picrylhydrazyl (DPPH) as standard ( $g = 2.0036$ ), and its spectrum was taken before and after each measurement. The operation conditions are given in Table 1 for both RT and low temperature. Signal intensities were measured directly from recorded first derivative spectra. Spectrum area under absorption curves, which is proportional to the total radical amounts, was calculated by double integration technique using Bruker WINEPR program [19]. Sample temperature inside the microwave cavity was monitored with a digital temperature control unit (Bruker ER 411-VT).

### 3 Results and Discussion

While unirradiated samples presented no ESR signal, irradiated polycrystalline of two compounds of CA were observed to present an ESR spectrum consisting of many strong and weak resonance lines (Fig. 1a, b). The ESR signals of radiation-induced radicals were strongly overlapped especially at the center of the experimental ESR spectrum. The weak resonance lines, which were located at both sides of the central lines, were less disturbed by lines than the central lines. RT spectra were calculated to spread over a magnetic field range of about 12 and 13 mT for anhydrous and monohydrate CA, respectively, and centered about  $g = 2.0032$ . The variations of the assigned line intensities  $I_1$ ,  $I_2$ ,  $I_3$  and  $I_4$  (Fig. 1a, b) and the spectrum area calculated by double integration technique for both monohydrate and

**Table 1** The spectrometer operation conditions adopted during the experiments

|                                 | RT           | Below RT     |
|---------------------------------|--------------|--------------|
| Central field (mT)              | 347.0        | 334.0        |
| Scan range (mT)                 | 15.0         | 15.0         |
| Microwave power (mW)            | 0.4          | 0.02         |
| Microwave frequency (GHz)       | $\sim 9.798$ | $\sim 9.422$ |
| Receiver gain ( $\times 10^4$ ) | 2.52         | 0.20         |
| Modulation frequency (kHz)      | 100          | 100          |
| Modulation amplitude (mT)       | 0.1          | 0.1          |
| Time constant (ms)              | 327.68       | 327.68       |
| Sweep time (s)                  | 83.89        | 83.89        |

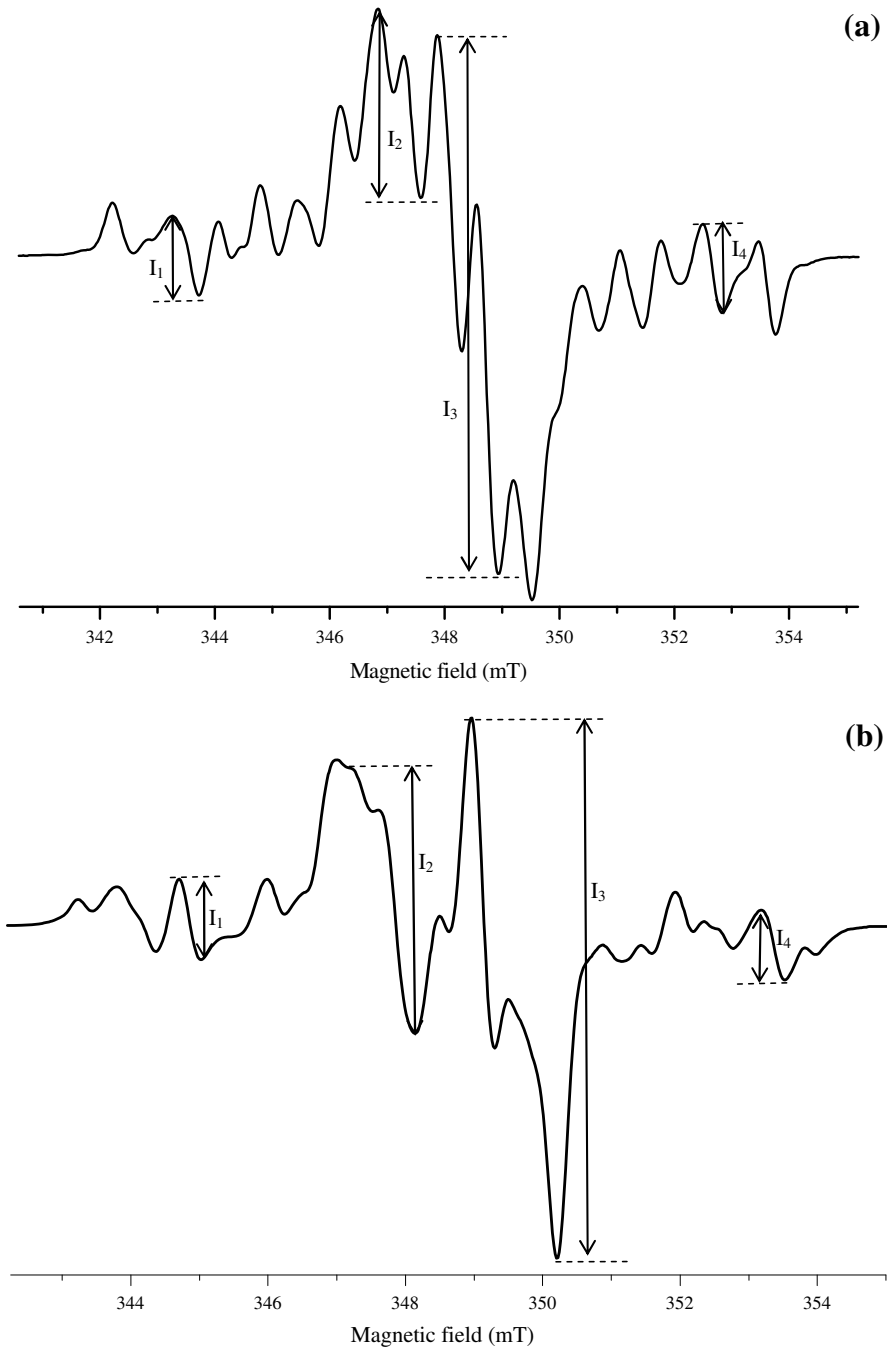


**Fig. 1** Room temperature ESR spectra of two CA compounds recorded under the same spectrometer setting conditions, and monitored intensities. **a** Monohydrate CA, **b** anhydrous CA irradiated at a dose of 10 kGy

anhydrous CA, with microwave power, applied dose, storage time and temperature were investigated.

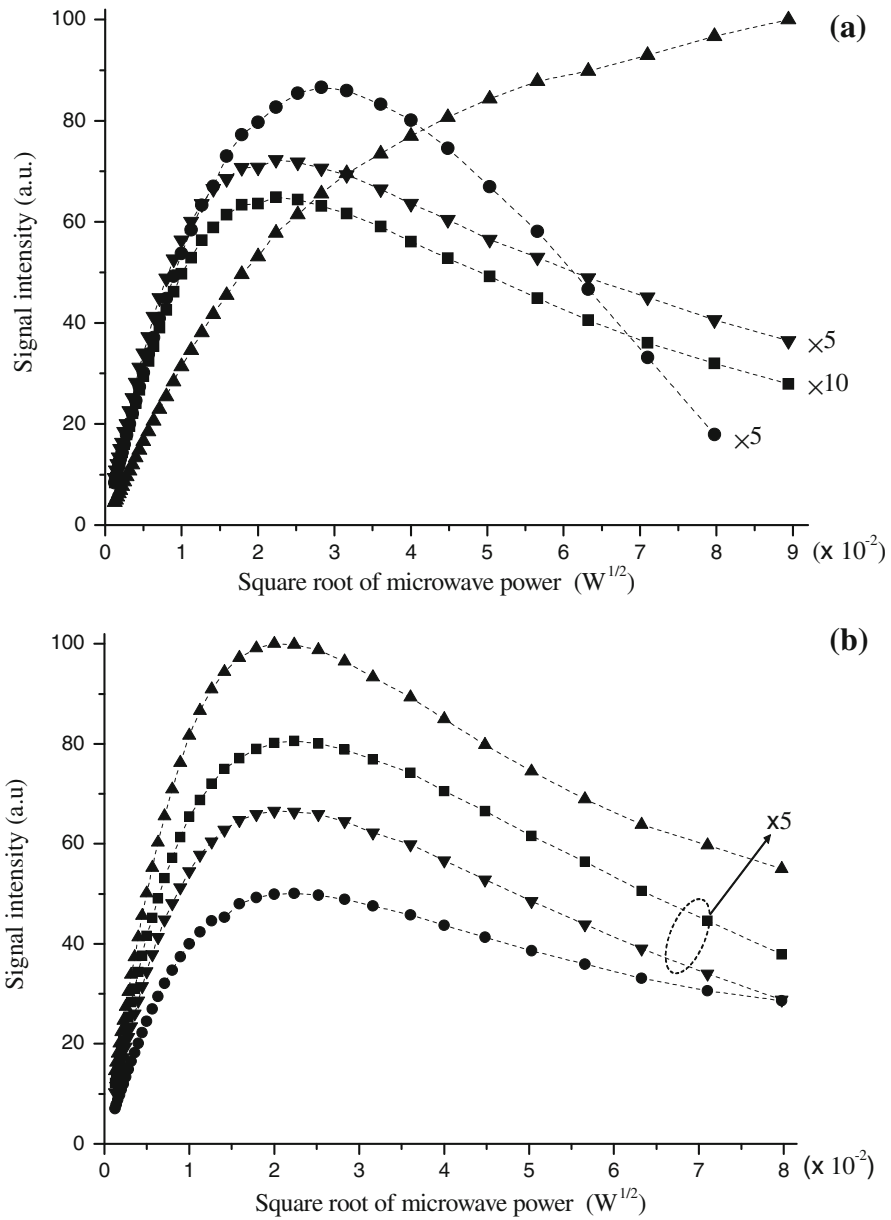
### 3.1 Variations of the Signal Intensities with Microwave Power

Samples irradiated at a dose of 10 kGy were used to determine the microwave power saturation features of associated radical species, and also to determine the spectrometer conditions that are used in the present study (Table 1). Variation of the assigned line intensities with microwave power was investigated both at RT and at 120 K in the range of  $1.6 \times 10^{-3} - 12.7$  and  $3.2 \times 10^{-4} - 2.5$  mW, respectively. Saturation results obtained for monitored  $I_1$ ,  $I_2$ ,  $I_3$ , and  $I_4$  intensities at RT are given in Fig. 2a, b for monohydrate and anhydrous CA, respectively. In the figure, some of the signals that have weak intensities were amplified 5 or 10 times to make them more visible and to make a comparison. The line intensities of the same compound were observed to have the same saturation behavior at 290 and 120 K but at lower microwave power values. This difference in the microwave power value is consistent with the Raman process. It is seen that the measured intensities of both compounds of CA present the features of homogeneously broadened resonance lines except the  $I_3$  intensity of monohydrate CA. It shows the features of inhomogeneously broadened resonance line.

### 3.2 Spectrum Simulation

A model based on the presence of three radical species with different spectroscopic parameters, which are denoted as radical I and III by Finch et al. [16], and another radical denoted as radical IV were used to describe the experimental ESR spectra by spectrum simulation in this study. In our investigations, we assume that the latter radical has the same structure of the radical III as proposed by Zeldes and Livingston [17] (see Table 2). ESR signal intensity data derived from the sample irradiated at 10 kGy were used to determine the spectroscopic parameters of the produced radical species. The spectroscopic parameters and percent concentration of these three radicals were calculated using a homemade simulation program and the results of both compounds of CA are given in Table 2. The theoretical sum spectrum and the spectrum of each individual radical of monohydrate and anhydrous CA are shown in Figs. 3 and 4, respectively, together with their experimental counterpart for comparison.

The spectroscopic parameters presented in Table 2 for the radicals of both CA compounds were found to be in a good agreement with that given in the literature [16, 17] except some differences in the hyperfine constants. The following findings related to the interaction of the unpaired electrons of each radical were observed: The unpaired electron of the radical I was found to interact with inequivalent four  $\beta$ -protons as given in the literature. The radical III interact with one  $\alpha$ -proton and three inequivalent  $\beta$ -protons. One of the  $\beta$ -protons has a hyperfine splitting smaller than the linewidth. Thus, it is accepted that the radical III interact with one  $\alpha$  and two inequivalent  $\beta$ -protons (Table 2). The other radical denoted as radical IV was

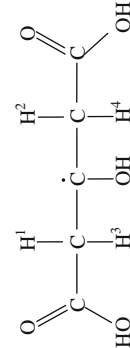
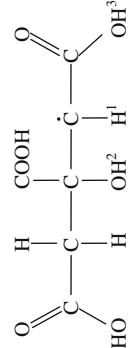
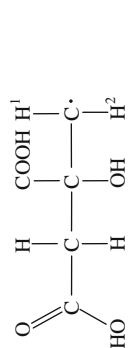


**Fig. 2** Microwave saturations of the monitored intensities at 290 K for a sample irradiated at a dose of 10 kGy. **a** Monohydrate CA, **b** anhydrous CA (filled square  $I_1$ ; filled circle  $I_2$ ; filled triangle  $I_3$  and filled inverted triangle  $I_4$ )

found to interact with two protons. These two couplings were found to be equal in monohydrate CA and slightly different in anhydrous CA (Table 2).



**Table 2** Spectroscopic parameters calculated for contributing radical species produced upon irradiation of anhydrous and monohydrate CA

| Radical  | Relative weight (%)                    | Linewidth $\Delta H_{pp}$ (mT)       | g value                                      | Hyperfine splitting (mT)   |
|--|--|--------------------------------------|--|--|
|  <p>(I)</p>   | <p>13.59 ± 1.86<br/>(41.57 ± 5.28)</p> | <p>0.54 ± 0.03<br/>(0.59 ± 0.05)</p> | <p>2.0037 ± 0.0005<br/>(2.0029 ± 0.0007)</p> | <p>H<sup>1</sup> 5.47 ± 0.04 (4.51 ± 0.11)<br/>H<sup>2</sup> 3.08 ± 0.04 (2.65 ± 0.11)<br/>H<sup>3</sup> 1.57 ± 0.04 (1.37 ± 0.11)<br/>H<sup>4</sup> 0.79 ± 0.04 (0.74 ± 0.11)</p> |
|  <p>(III)</p> | <p>20.62 ± 1.05<br/>(46.29 ± 4.43)</p> | <p>0.40 ± 0.02<br/>(0.48 ± 0.03)</p> | <p>2.0039 ± 0.0006<br/>(2.0048 ± 0.0007)</p> | <p>H<sup>1</sup> 1.83 ± 0.03 (1.89 ± 0.09)<br/>H<sup>2</sup> 0.67 ± 0.03 (0.64 ± 0.09)<br/>H<sup>3</sup> 0.47 ± 0.03 (0.37 ± 0.09)</p>   |
|  <p>(IV)</p>  | <p>65.79 ± 4.71<br/>(12.14 ± 5.22)</p> | <p>1.47 ± 0.16<br/>(0.40 ± 0.03)</p> | <p>2.0027 ± 0.0006<br/>(2.0040 ± 0.0007)</p> | <p>H<sup>1</sup> 0.84 ± 0.02 (0.69 ± 0.02)<br/>H<sup>2</sup> 0.84 ± 0.02 (0.47 ± 0.02)</p>   |

Values in parenthesis are the spectroscopic parameters of anhydrous CA

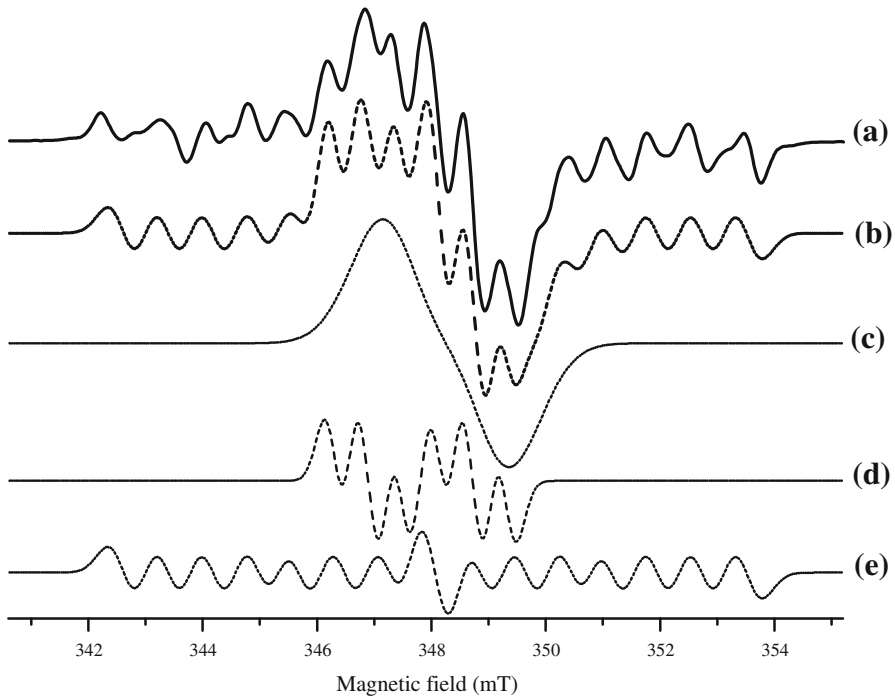


**Fig. 3** Experimental (*solid line*) and theoretical (*dashed lines*) ESR spectra of monohydrate CA calculated using parameter values given in Table 2. **a** Experimental spectra, **b** sum spectra, **c** spectra of radical IV, **d** spectra of radical III, and **e** spectra of radical I

### 3.3 Kinetic Studies

Radical stability at RT is one of the most important parameters in ESR dosimetry and in discrimination of irradiated samples from unirradiated ones. A sample irradiated at a dose of 10 kGy was stored at RT open to air (the average relative humidity is below 55 %), and its spectra were recorded at a regular time intervals over a storage period of 90 days. Collected decay data relevant to the resonance line that has the highest intensity ( $I_3$ ) and spectrum area were presented (Fig. 5). As it is seen,  $I_3$  and spectrum area decays but with different rates in monohydrate CA (Fig. 5). The radicals that were produced in anhydrous CA do not decay as fast as in monohydrate CA, and after the end of 3 months only 20 % of the total number of the radicals was decayed (inset Fig. 5). The fitting functions and the calculated parameters were given in the figure both for the spectrum area ( $N$ ) and  $I_3$ .

Variations of the line intensities above the RT were also studied to get information about high temperature decay kinetics of the radicals produced in  $\gamma$ -irradiated anhydrous and monohydrate CA. Annealing studies were performed at temperatures 370, 390, 400 and 410 K, and 310, 315, 320 and 330 K for an annealing period of 60 min of anhydrous and monohydrate CA, respectively. These differences in the annealing temperatures of both compounds implied that the

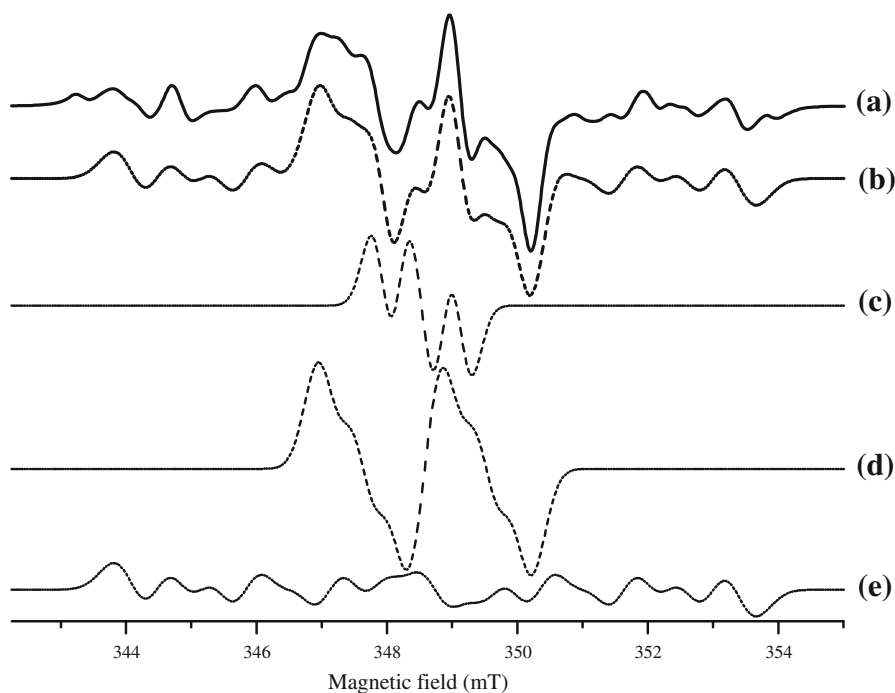


**Fig. 4** Experimental (*solid line*) and theoretical (*dashed lines*) ESR spectra of anhydrous CA calculated using parameter values given in Table 2. **a** Experimental spectra, **b** sum spectra, **c** spectra of radical IV, **d** spectra of radical III, and **e** spectra of radical I

activation energies of anhydrous CA should be higher than monohydrate CA. Intensities were normalized to the intensities measured from the first spectrum recorded 5 min after positioning the sample in the microwave cavity, to establish initial thermal equilibrium. Variations of the spectrum area at the annealing temperatures of anhydrous and monohydrate CA are given in Fig. 6a, b. While only 5 % of the total number of radicals in irradiated monohydrate CA decays during annealing at 310 K, above 310 K the radicals started to decay rapidly even after 10 min of annealing (Fig. 6a). Measurements of the spectrum area were used to determine the decay constant of the radicals produced after the irradiation of monohydrate CA.

In agreement with the literature and spectrum simulation, measured high temperature annealing data of the spectrum area of anhydrous and monohydrate CA were fitted to a function comprising three exponentially decaying functions of time of different weights and different decay constants ( $k$ s) representing the contributions of three radical species. Activation energies of the involved species of both CA compounds were calculated from  $\ln(k) - T^{-1}$  graphs and values presented in Table 3 were obtained. Derived decay constants were used to calculate the theoretical variations of the measured quantities. The results related to spectrum area are presented in Fig. 6a and b. It is seen that calculated decay constant describes fairly well the variations of spectrum area of anhydrous and monohydrate

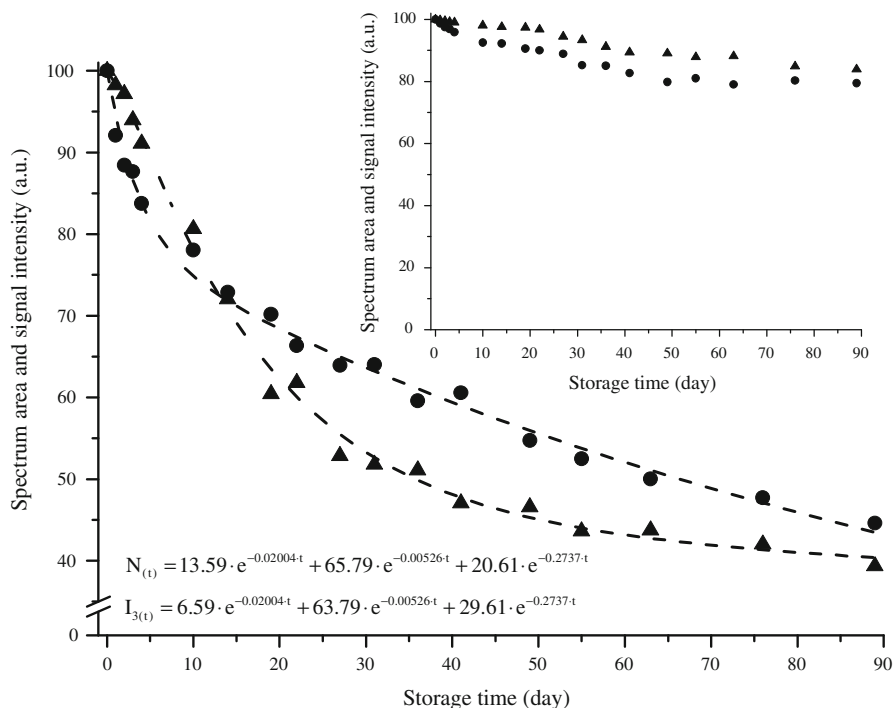


**Fig. 5** Variations of the signal intensity  $I_3$  and spectrum area with storage time at RT for monohydrate CA. Symbols experimental (filled triangle  $I_3$  and filled circle spectrum area), dashed lines calculated (inset anhydrous CA)

CA at the annealing temperatures. This was also the case for its measured line intensities. As it is expected the activation energies of the radical that produced in anhydrous CA are found to be higher than monohydrate CA (Table 3).

### 3.4 Dose–Response Curves

Dosimetric potentials of anhydrous and monohydrate CA were explored through the variations of the assigned resonance line intensities and spectrum area with the applied radiation dose. Samples irradiated to doses of 0.5, 1, 2, 5, 7, 10, 15 and 20 kGy were used to construct experimental dose–response curves. Four different functions of the applied dose that given in Table 4 (linear, linear + quadratic, power, and exponential) have been tried to describe experimental dose–response data without forcing them to pass through the origin. In these functions (Table 4),  $I$  and  $D$  stand for the ESR line intensity/spectrum area and absorbed dose in kGy, respectively, and  $a, b, c, \dots$  are the constants to be determined. Intensities and spectrum area normalized to the receiver gain and to the mass of the sample were used in the calculations. The data of the intensity  $I_3$  and spectrum area are presented in Fig. 7 for each CA compound (right y axis spectrum area, and left y axis signal intensity). It is seen that while the variations of the spectrum area with the applied

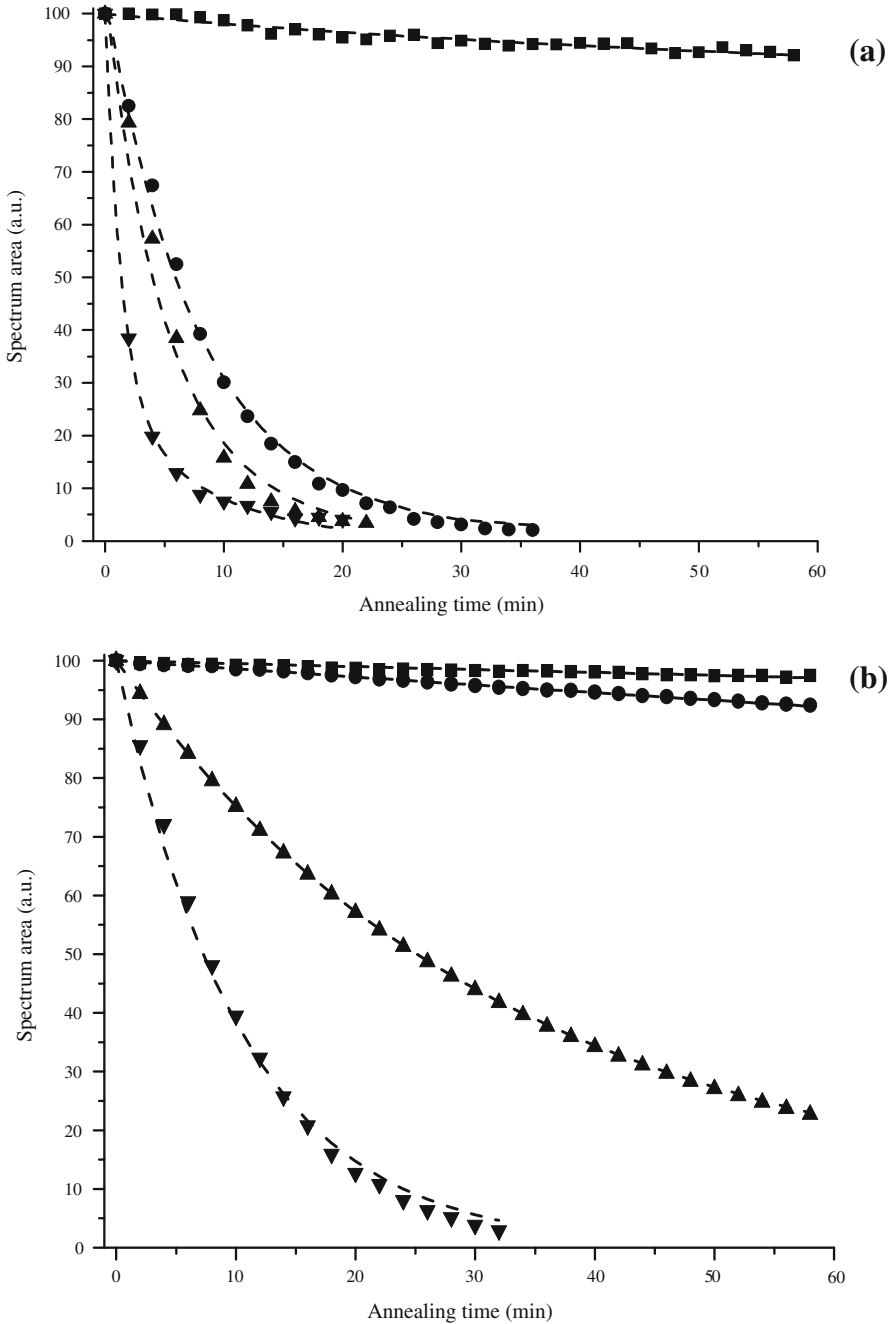


**Fig. 6** Variation of the spectrum area of CA compounds with annealing time at different temperatures. **a** Monohydrate CA (filled square 310 K, filled circle 315 K, filled triangle 320 K, filled inverted triangle 330 K) and **b** anhydrous CA (filled square 370 K, filled circle 390 K, filled triangle 400 K, filled inverted triangle 410 K)

**Table 3** Activation energies calculated for responsible radical species using the finding from annealing study

| Radical species | Activation energy (kJ/mol) |                |
|-----------------|----------------------------|----------------|
|                 | Monohydrate CA             | Anhydrous CA   |
| I               | 159.18 ± 21.38             | 426.15 ± 12.48 |
| III             | 95.62 ± 18.42              | 463.61 ± 13.74 |
| IV              | 11.82 ± 3.47               | 167.28 ± 9.61  |

**Table 4** Mathematical functions, parameter values and correlation coefficients best describing experimental dose–response data

| Functions                          | Monohydrate CA |                  | Anhydrous CA   |                  |                 |
|------------------------------------|----------------|------------------|----------------|------------------|-----------------|
|                                    | Spectrum area  | $I_3$            | Spectrum area  | $I_3$            |                 |
| $I = a + b \cdot D$                | a              | 7.723 ± 0.043    | 2.498 ± 0.083  | -2.437 ± 0.043   | 2.412 ± 0.074   |
|                                    | b              | 14.315 ± 0.031   | 1.884 ± 0.078  | 10.685 ± 0.025   | 2.909 ± 0.060   |
|                                    | r <sup>2</sup> | <u>0.98977</u>   | 0.97481        | <u>0.99757</u>   | 0.99015         |
| $I = c + f \cdot D + g \cdot D^2$  | c              | -0.749 ± 0.040   | 0.666 ± 0.055  | -1.173 ± 0.062   | 0.448 ± 0.061   |
|                                    | f              | 17.825 ± 0.058   | 2.643 ± 0.063  | 10.161 ± 0.053   | 3.722 ± 0.083   |
|                                    | g              | -0.180 ± 0.060   | -0.039 ± 0.013 | 0.027 ± 0.011    | -0.042 ± 0.053  |
|                                    | r <sup>2</sup> | 0.99455          | 0.98754        | 0.99776          | 0.99638         |
| $I = h \cdot D^k$                  | h              | 20.440 ± 0.248   | 3.793 ± 0.386  | 9.398 ± 0.198    | 4.765 ± 0.429   |
|                                    | k              | 0.883 ± 0.142    | 0.775 ± 0.240  | 1.041 ± 0.241    | 0.839 ± 0.117   |
|                                    | r <sup>2</sup> | 0.99351          | 0.98766        | 0.99766          | 0.99678         |
| $I = m \cdot (1 - e^{-n \cdot D})$ | m              | 7880.781 ± 3.043 | 61.329 ± 0.843 | 8250.094 ± 2.830 | 122.934 ± 0.953 |
|                                    | n              | 0.002 ± 0.001    | 0.048 ± 0.011  | 0.002 ± 0.001    | 0.032 ± 0.013   |
|                                    | r <sup>2</sup> | 0.98811          | <u>0.98798</u> | 0.99680          | <u>0.99674</u>  |

Functions that have the correlation coefficient underlined are used to construct the dose–response curves

dose are almost linear, the variations of  $I_3$  exhibit rather exponential variations in the investigated dose range (0.5–20 kGy) for both anhydrous and monohydrate CA. Parameter values calculated for the functions proposed to describe the experimental dose–response data are presented in Table 4.

### 4 Conclusions

Irradiation with  $\gamma$ -ray produces defects which are generally detectable by ESR spectroscopy. Irradiated anhydrous and monohydrate CA compounds have different ESR spectra. However, while the radicals produced upon the irradiation of both compounds have the same structure their spectroscopic parameters are different due to the difference of the crystal configurations. The investigations indicate that a model based on the presence of three radical species, denoted as I, III and IV of

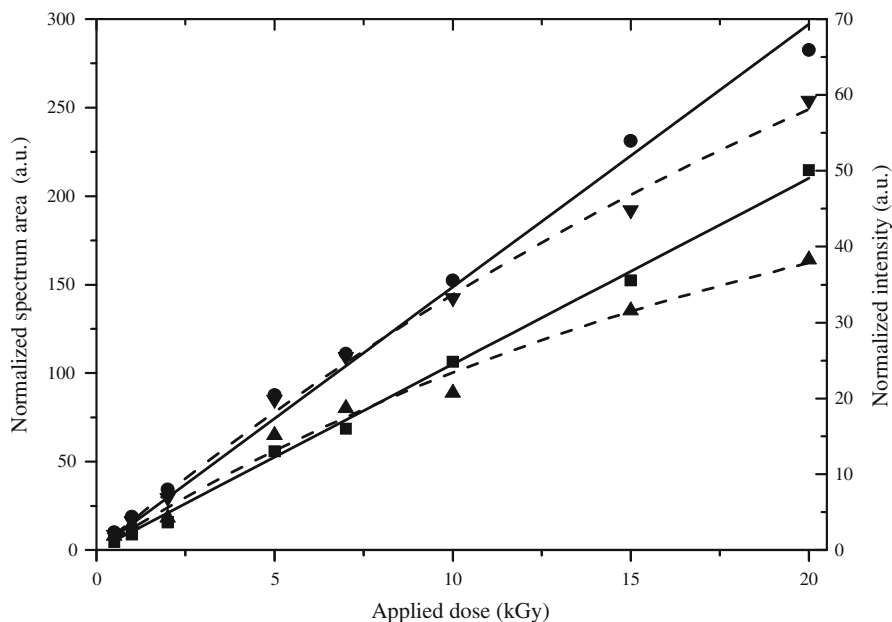


**Fig. 7** Variations of the measured intensity  $I_3$  (filled triangle monohydrate CA and filled inverted triangle anhydrous CA) and spectrum area (filled circle monohydrate CA and filled square anhydrous CA) with applied radiation dose. Symbols experimental, lines calculated data using exponential and linear function for the intensities (dashed lines) and spectrum areas (solid lines), respectively

different spectroscopic and decay features were found to describe well the experimental results derived in the present work.

The microwave saturation behavior of the monitored intensities of both CA compounds was investigated at RT and at 120 K. It is found that they present the features of homogeneously broadened resonance lines except the  $I_3$  intensity of monohydrate CA. As it is seen from the spectrum simulations of both compounds, the radical I is responsible for the monitored lines  $I_1$  and  $I_4$ . Furthermore, lines  $I_2$  and  $I_3$  have been contributed from the three radicals with different relative contribution (Figs. 3, 4). These different contributions of the individual spectra of the radicals and the overlapping of the signals which affect the shape and the resolution of the interested lines are probably caused to the different line broadening [20].

The radicals of irradiated monohydrate CA decay relatively fast above the RT. Above 315 K almost the total number of radicals decays in 15 min of annealing. Decay of anhydrous CA compound is not as fast as monohydrate CA. Anhydrous CA starts decaying at about 400 K. Thus, the activation energies of anhydrous CA were calculated to be 4–10 times higher than that of monohydrate CA (see also Table 3). While about 60 % of the radicals of monohydrate CA decay in the period of 3 months, only 20 % of the radicals of anhydrous CA decay in the same period at RT.

An alternative material to be used as high dose ESR dosimeter should have a high radical yield, a linear dose–response curve of both the spectrum area and the ESR

lines, sharp spectral lines, stable radical at RT [21, 22] and simple ESR spectra. In addition, its dosimetric features should be comparable with alanine. In this respect, the dosimetric features of each compound were summarized as follows: although the decay of monohydrate CA is fast at RT and high temperature, the slow decay of anhydrous CA at the same temperatures make it more suitable to be a candidate of dosimetric material than monohydrate CA. In addition, the dose–response curve related to the spectrum area of anhydrous and monohydrate CA shows a linear variation with the applied radiation dose in the range of 0.5–20 kGy. The variation of the spectrum areas of both the compound show that the radiation yields of anhydrous CA is higher than monohydrate CA. While these are the positive features for a good candidate of a dosimetric material, the complex ESR spectrum and the exponential decay behavior of the main ESR lines (etc.  $I_3$ ) with the radiation dose seem to be negative features. It is concluded that while some of the dosimetric features of both CA compounds are compatible to be a dosimetric material, there are also some negative features. Despite all the negative findings from the ESR spectrum and decay, ESR spectroscopy could be used for the discrimination of irradiated CA from unirradiated one even after a storage period of 3 months.

## References

1. C.R. Soccol, L.P.S. Vandenberghe, C. Rodrigues, A. Pandey, *Food Technol. Biotechnol.* **44**, 141–149 (2006)
2. G.S. Dhillon, S.K. Brar, M. Verma, R.D. Tyagi, *Food Bioprocess Technol.* **4**, 505–529 (2010)
3. Y. Jiang, L. Pen, J. Li, *J. Food Eng.* **63**, 325–328 (2004)
4. L.M. Sammel, J.R. Claus, *Meat Sci.* **72**, 567–573 (2006)
5. B. Aliakbarian, F. Dehghani, P. Perego, *Food Chem.* **116**, 617–623 (2009)
6. C.A. Hall, S.L. Cuppett, in *Antioxidant methodology: in vivo and in vitro Concepts*, ed. by O.I. Aruoma, S.L. Cuppett (AOCS press, Champaign, 1997), p. 141
7. S. Barrington, J.S. Kim, L.J.W. Wang Kim, *Korean J. Chem. Eng.* **26**, 422–427 (2009)
8. Y.X. Chen, Q. Lin, Y.M. Luo, Y.F. He, S.J. Zhen, Y.L. Yu, G.M. Tian, M.H. Wong, *Chemosphere* **50**, 807–811 (2003)
9. J. Yang, A.R. Webb, G.A. Ameer, *Adv. Mater.* **16**, 511–516 (2004)
10. H. Namazi, H. Adeli, *Biomaterials* **26**, 1175–1183 (2005)
11. I. Djordjevic, N.R. Choudhury, N.K. Dutta, S. Kumar, *Polymer* **50**, 1682–1691 (2009)
12. A.T. Naeini, M. Adeli, M. Vossoughi, *Nanomedicine* **6**, 556–562 (2010)
13. C.E. Nordman, A.S. Weldon, A.L. Petterson, *Acta Cryst.* **13**, 418–426 (1960)
14. J.P. Glusker, J.A. Minker, A.L. Petterson, *Acta Cryst. B* **25**, 1066–1072 (1969)
15. G. Roelofsen, J.A. Kanters, *Cryst. Struct. Commun.* **1**, 23–26 (1972)
16. L.L. Finch, J.E. Johnson, G.C. Moulton, *J. Chem. Phys.* **70**, 3662–3668 (1979)
17. H. Zeldes, R. Livingston, *J. Am. Chem. Soc.* **93**, 1082–1085 (1971)
18. H. Tuner, M. Korkmaz, *Radiat. Environ. Biophys.* **49**, 723–729 (2010)
19. D. Barr, J.J. Jiang, R. Weber, Performing double integrations using WIN-EPR. Bruker biospin report 6. (1998)
20. J.A. Weil, J.R. Bolton, J.E. Wertz, *Electron paramagnetic resonance: elementary theory and practical applications*, 1st edn. (Wiley, New York, 1994), pp. 303–304
21. M. Ikeya, G.M. Hassan, H. Sasaoka, Y. Kinoshita, S. Takaki, C. Yamanaka, *Appl. Radiat. Isot.* **52**, 1209–1215 (2000)
22. A. Lund, S. Olsson, M. Bonora, E. Lund, H. Gustafsson, *Spectrochim. Acta A* **58**, 1301–1311 (2002)